

ADA 111 399

DTIC FILE COPY

UNCLASSIFIED
SECURITY CLASSIFICATION OF THIS PAGE (When Data Entered)

REPORT DOCUMENTATION PAGE		READ INSTRUCTIONS BEFORE COMPLETING FORM
1. REPORT NUMBER Technical Report No. 10	2. GOVT ACCESSION NO. AD-A111 399	3. REPORT'S CATALOG NUMBER ①
4. TITLE (and Subtitle) THE ROLE OF CHEMICAL BONDING IN GRAIN BOUNDARY EMBRITTLEMENT		5. TYPE OF REPORT & PERIOD COVERED Interim
6. PERFORMING ORG. REPORT NUMBER		7. CONTRACT OR GRANT NUMBER(s) N00014-79-C-0991
8. AUTHOR(s) R.P. Messmer and C.L. Briant General Electric Co. Cor. Research and Development Schenectady, NY 12301		9. PROGRAM ELEMENT, PROJECT, TASK AREA & WORK UNIT NUMBERS NR SRO-013/9-12-79 (472)
10. PERFORMING ORGANIZATION NAME AND ADDRESS Trustees of the University of Pennsylvania Office of Project Research and Grants 3451 Walnut Street Philadelphia, PA 19104-3859		11. REPORT DATE February 10, 1982
12. CONTROLLING OFFICE NAME AND ADDRESS Office of Naval Research Department of the Navy 500 N. Quincy St. Arlington, VA 22217		13. NUMBER OF PAGES 32
14. MONITORING AGENCY NAME & ADDRESS (if different from Controlling Office)		15. SECURITY CLASS. (of this report) Unclassified
16. DISTRIBUTION STATEMENT (of this Report) Approved for public release; distribution unlimited		15a. DECLASSIFICATION DOWNGRADING SCHEDULE
17. DISTRIBUTION STATEMENT (of the abstract entered in Block 20, if different from Report)		
18. SUPPLEMENTARY NOTES Preprint; accepted for publication in Acta Met.		
19. KEY WORDS (Continue on reverse side if necessary and identify by block number) Grain boundary embrittlement		
20. ABSTRACT (Continue on reverse side if necessary and identify by block number) Brittle intergranular fracture occurs when impurity elements segregate to the grain boundaries of a material and lower their cohesion strength. Although many embrittling elements have been identified by experimental studies, the reason why these elements cause embrittlement has remained elusive. This paper presents results of fully quantum mechanical cluster calculations which address this question. It will be shown that strong embrittling elements draw charge from neighboring metal atoms onto themselves. They thus remove charge		

DD FORM 1 JAN 73 1473

EDITION OF 1 NOV 65 IS OBSOLETE
S/N. 0102-014-6601UNCLASSIFIED
SECURITY CLASSIFICATION OF THIS PAGE (When Data Entered)

UNCLASSIFIED

UNCLASSIFIED EXCEPT WHERE SHOWN OTHERWISE

from the metal-metal bonds which hold the grain boundary together and weaken them. Cohesive enhancers do not draw charge off the metal atoms and thus do not weaken the metal-metal bond network. In addition, they form rather homopolar bonds with the metal atoms and thus provide an added increment of bonding in the grain boundary.

REF ID: A6062

OFFICE OF NAVAL RESEARCH

Contract N00014-79-C-0991

Task No. NR SRO-013

TECHNICAL REPORT NO. 10

The Role of Chemical Bonding in Grain Boundary Embrittlement

by

R.P. Messmer and C.L. Briant

Prepared for Publication

in

Acta Met

University of Pennsylvania
Office of Project Research and Grants
3451 Walnut Street
Philadelphia, Pennsylvania 19104-3859

February 10, 1982

Reproduction in whole or in part is permitted for any purpose of the
United States Government.

This document has been approved for public release and sale; its
distribution is unlimited.



82 02 26 024

Acta Met, in press

**THE ROLE OF CHEMICAL BONDING
IN GRAIN BOUNDARY EMBRITTLEMENT**

R. P. Messmer and C. L. Briant

**General Electric Company
Corporate Research and Development
P. O. Box 8
Schenectady, New York 12301**

- 4 -

ABSTRACT

Brittle intergranular fracture occurs when impurity elements segregate to the grain boundaries of a material and lower their cohesive strength. Although many embrittling elements have been identified by experimental studies, the reason why these elements cause embrittlement has remained elusive. This paper presents results of fully quantum mechanical cluster calculations which address this question. It will be shown that strong embrittling elements draw charge from the neighboring metal atoms onto themselves. They thus remove charge from the metal-metal bonds which hold the grain boundary together and weaken them. Cohesive enhancers do not draw charge off the metal atoms and thus do not weaken the metal-metal bond network. In addition, they form rather homopolar bonds with the metal atoms and thus provide an added increment of bonding in the grain boundary.

INTRODUCTION

Brittle intergranular fracture has been observed in many different materials. Particularly well-documented experiments have been reported for iron⁽¹⁻¹⁰⁾ and steels,⁽¹¹⁻²⁸⁾ nickel alloys,⁽²⁹⁻³²⁾ copper alloys,⁽³³⁻³⁶⁾ and refractory alloys.⁽³⁷⁻³⁸⁾ This mode of brittle fracture is also often concurrent with a greatly reduced fracture toughness. Consequently, the possibility of its occurrence has limited the application of many alloys, and its unexpected occurrence in practice has often caused catastrophes.

Although the details of brittle intergranular fracture depend on the specific material and application, one observation holds for all known cases. Impurities which have a low solubility in the bulk segregate to the grain boundaries and locally lower the cohesive strength of the metal. These embrittling elements are termed impurities because their bulk concentrations are often below the level of control in commercial melting practices (e.g., less than 200 ppm). However, when these elements are segregated to the grain boundaries, their concentrations at these interfaces can be very high, possibly five to ten atomic percent.

A problem such as this is very complex. The full process of intergranular fracture undoubtedly involves dislocation motion and pile ups, plastic deformation, work hardening and bond breaking. In this paper we focus on the chemical bonding aspect of this problem. If we can understand why the segregated impurities weaken the bonding at the grain boundaries, then we will be one step closer to a complete description of intergranular fracture.

There are a number of pieces of experimental evidence which show that the segregated impurities weaken the bonds at the grain boundary. First, the segregation causes a transition of the brittle fracture mode from crystallographic cleavage to intergranular fracture. Therefore, the grain boundaries have become weak, relative to the cleavage plane. Secondly, the ductile-to-brittle transition temperature in body-centered-cubic metals increases with increasing segregation and intergranular fracture. Therefore, as a result of the decreased bond strength, a brittle crack can propagate at high temperatures. Finally, the fracture energy decreases as the amount of segregation

increases.

Several qualitative explanations have been offered to suggest how this weakening might occur.^(12,14,38,40) First, it has been noted that the embrittling elements are often from groups IV to VI of the periodic table. Second, it has been shown that the embrittling power of the element increases as one moves from group IV to VI in a given row of the periodic table. Therefore, impurities which are more electronegative with respect to their transition metal hosts are stronger embrittlers. One might expect that the greater the difference in electronegativity, the more disruptive the impurity would be on bonds at the grain boundary. Also for a given electronegativity, a larger atom is a more potent embrittler than a smaller one. This effect presumably results from strains produced by the impurity.⁽¹²⁾ Finally, it has been observed that carbon in iron^(2,5,10,41) and boron in nickel⁽²⁹⁾ reduce embrittlement.

In order to understand the chemical bonding aspect of grain boundary embrittlement at its most fundamental level, it is necessary to perform fully quantum mechanical calculations which will describe the bonding at the grain boundary. Because one is interested in the local chemistry at the boundary, a molecular orbital cluster approach is particularly advantageous. One can then calculate the chemical bonding for clusters which have atomic arrangements representative of those of the grain boundary and determine changes in the bonding which occur when an embrittling element is introduced. Recently, we reported the first such calculations.⁽⁴²⁾ We used the X- α self-consistent-field scattered-wave method of Slater⁽⁴³⁾ and Johnson⁽⁴⁴⁾ and applied it to a cluster model relevant to the embrittlement of nickel by sulfur. In this paper we extend these calculations to other systems. We will show that the strongly embrittling elements are indeed very electronegative with respect to the host metal and draw charge from the metal atom onto themselves. Thus the metal-impurity bond is heteropolar. In contrast, a cohesive enhancer such as boron in nickel does not deplete the metal atoms of charge and the impurity-metal bond is much more homopolar. Such an element will then provide additional bonding at the grain boundary while not destroying the metal-metal bonds. In contrast, we suggest that carbon is a rather benign impurity but not a cohesive enhancer, and that the beneficial effects of carbon additions

to iron result from its displacing a more potent embrittler such as sulfur from the boundary.

METHOD

The application of the molecular orbital cluster method to the problem of grain boundary embrittlement involves the specification of a technique for calculating the molecular orbitals together with a choice of the atomic arrangement of atoms in the cluster which simulate the local structure at the grain boundary.

The determination of appropriate atomic arrangement in the cluster has been greatly facilitated by recent work which shows that the structure of grain boundaries can be described in terms of polyhedral units in which atoms are placed at vertices.^(45,46) These polyhedra, which are quite similar to the Bernal deltahedra, can then be used as the clusters in the calculations. In this paper we have used the simplest grain boundary polyhedron, the tetrahedron, Figure 1. In these calculations the impurity atom is placed at the center of the tetrahedron and surrounded by the four metal atoms.

The technique we have used for calculating the molecular orbitals is the self-consistent-field X- α scattered-wave theory. This cluster method has been applied with great success to many problems where local bonding is of overriding importance such as chemisorption^(47,48) and amorphous metals.⁽⁴⁹⁾ Three types of information obtained from such calculations have been employed in this study. They are the following: the orbital energy level diagrams, the one-electron molecular orbital wave functions, and the valence electron charge density of the atoms in the cluster. The latter two can be presented graphically as equi-valued contour plots.

The results of calculations on five different clusters are reported in this paper. In three of these clusters Fe is the host metal, and in two Ni is the host, Table 1. We have chosen these systems because they have been studied experimentally and represent a range of embrittlement potency. Sulfur is a strong embrittler of both Fe^(2-5,7,8) and Ni,⁽²⁹⁻³²⁾ P is a weak embrittler of iron,⁽⁴⁾ and C^(2,5) and B⁽²⁹⁾ have been reported to counteract the sulfur

induced embrittlement in Fe and Ni, respectively.

The calculations performed on these clusters were fully spin polarized so that any magnetic effects would be accounted for. As would be expected, the iron clusters had a much greater magnetic moment than did the nickel clusters. This result is a consequence of the fact that the iron clusters have many more unpaired spins than the nickel clusters which arises from the larger difference in energy of a given level between the spin up (the majority spin) and spin down components in the iron clusters as compared to the Ni clusters.

RESULTS

Figures 2-6 show the energy level diagrams for the five clusters. The levels are designated by the irreducible representations of the tetrahedral point group under which their corresponding orbital wave functions transform. Particular attention should be paid in these diagrams to the $1a_1$ and $1t_2$ levels. These two levels correspond to the wave functions which describe the metal-impurity interaction. The $1a_1$ orbital contains the contribution from the impurity valence s electrons and the $1t_2$ orbital contains the contribution from the impurity p electrons. All other energy levels correspond to wave functions which are located either completely or almost completely on the metal atoms. We see that the $1a_1$ and $1t_2$ levels are the lowest two energy levels in each cluster. Also there is a significant energy difference between either of these levels and the closely spaced group of levels that lie above them. This difference is greatest for the sulfur containing clusters, less so for Fe_4P and Fe_4C , and least of all Ni_4B . We might then expect that as this difference increases, the wave functions which correspond to these two levels will be located more on the impurity atom and less on the metal atoms.

There is a very simple way in which one can understand the qualitative effects which might be expected to occur by considering the interaction of the metal with the impurity series B, C, P, S. First consider the 2s and 3s valence orbital energies of the impurities B, C and P, S, respectively. These orbital energies are all below the mean of the orbital energies of the metal. As one goes through the series B, C, P, S, the difference between the orbital energy of the impurity and those of the metal continue to increase. Thus

$E_I^0 - E_M^0$ continues to increase in magnitude (recall however that orbital energies are negative quantities) for this series of impurities. The quantities E_I^0 and E_M^0 refer to the orbital energies of the isolated impurity and metal respectively.

If one then investigates the interaction of the metal cluster and the impurity by perturbation theory, a procedure which has validity in discussing qualitative effects, but certainly not quantitative aspects, one can write the perturbed wave function of the impurity as

$$\Psi_I = \Psi_I^0 + \frac{V}{E_I^0 - E_M^0} \Psi_M^0 \quad (1)$$

This shows that the perturbation, which causes an interaction energy V (which is attractive, and hence negative) mixes the unperturbed wave function of the impurity with those of the metal. Both the numerator and denominator of the second term in Eq. (1) are negative, hence a bonding-like interaction occurs. If one assumes that V is roughly constant for the series of impurities B, C, P and S, then the denominator of the second term will control the mixing of the unperturbed impurity and metal wave functions. As mentioned above, the magnitude of the factor in the denominator increases for the series of impurities and thus one expects much less of a metal contribution in Eq. (1) for a sulfur impurity than for the case of the B impurity. One can make a similar argument for the case of the impurity p-orbitals interacting with the metal.

This idea is verified when we examine the contour plots which correspond to these two orbitals. These plots are shown in Figures 7-11; the cross section is taken in the cross-hatched plane of Figure 1 so that it includes two metal-metal atoms and the impurity. The plots for Fe_4S and Ni_4S are shown in Figures 7 and 8, respectively. For these two clusters the $1a_1$ orbitals have practically no metal content for either the spin up or spin down case. The $1t_2$ orbitals also have little content on the metal atoms and are more concentrated on the impurity. One other fact should be noted from these plots. Because the nickel cluster has a small magnetic moment, the energies of the spin up $1t_2^{\uparrow}$ and spin down $1t_2^{\downarrow}$ levels are quite similar and the orbitals which

correspond to these energies are similar. However, in the iron cluster which has a large magnetic moment, the spin up and spin down energy levels have different energies and the corresponding wave functions are also different. Therefore, we see in Figure 7 that the $1t_2^{\uparrow}$ orbital has more metal atom content than does its $1t_2^{\downarrow}$ counterpart.

Similar plots for Fe_4P are shown in Figure 9. Both the $1a_1$ and $1t_2$ orbitals have more metal atom content and are less localized on the impurity atom than for Fe_4S and Ni_4S . The results for Fe_4C , Figure 10, appear quite similar to the results for Fe_4P . Finally, the results for Ni_4B are shown in Figure 11. It is clear that the $1a_1$ and $1t_2$ wave functions of this cluster have the most metal content and are least localized on the impurity atom. Therefore, as we go from the strong embrittler S in both Fe and Ni to the cohesive enhancer of B in Ni, the wave functions which describe the impurity-metal bonds go from being highly localized on the impurity atom with little content on the metal atom to being much more equally distributed between the impurity and the metal. The bonds which actually form should then vary from being heteropolar in the case of the strong embrittlers with the negative charge concentrated on the impurity, to being much more homopolar in the case of cohesive enhancers.

To observe this directly we have used the wave functions to calculate the valence charge density. The charge density $\rho(\vec{r})$ is usually obtained by summing over the square of all the wave functions. That is,

$$\rho(\vec{r}) = \sum_j n_j \phi_j^*(\vec{r}) \phi_j(\vec{r}) \quad (2)$$

where the $\phi_j(\vec{r})$ are the molecular orbitals of the system and n_j is the occupation number of the j th orbital. However, since only a limited number of these orbitals ($1a_1^{\uparrow}$, $1a_1^{\downarrow}$, $1t_2^{\uparrow}$, $1t_2^{\downarrow}$, $4t_2^{\uparrow}$, $4t_2^{\downarrow}$) contribute to the impurity-metal bond, we can define a special charge density $\rho_{IM}(\vec{r})$ which includes only these orbitals.

$$\rho_{IM}(\vec{r}) = \sum_{I-M} n_j \phi_j^*(\vec{r}) \phi_j(\vec{r}) \quad (3)$$

The results of these calculations are shown in Figure 12. Just as would be expected from the wave function plots, the charge density is much greater on the impurity atom than on the metal atoms for the Fe_4S and Ni_4S clusters. As we move to Fe_4P and Fe_4C , and then on to Ni_4B , the charge becomes much more equally distributed between the impurity and the host metal atoms. This fact is most clearly observed in these plots by examining the sixth contour, which is darkened in the plots in Figure 12. In the sulfur containing clusters it is broken into two parts, one around each metal atom and one around the sulfur; in the other clusters it is continuous around the metal and impurity atoms. As expected, the strong embrittlers are very electronegative with respect to their metal host whereas the cohesive enhancers are not, and the transition from a heteropolar bond to a homopolar bond as embrittling potency decreases is clearly evident.

DISCUSSION

The major result of the previous section was the following. When an impurity atom is placed in a cluster of host metal atoms, one can distinguish that different types of bonds are forming. For a strong embrittler such as S in Ni or Fe, the bonds which form are such that charge is concentrated very heavily on the impurity atoms and very little on the metal atoms. The embrittling element is electronegative with respect to the metal and the heteropolar bond which forms could be approximately described as being ionic. In contrast, for a cohesive enhancer such as B in Ni, the charge is much more equally shared between the host-metal and impurity. Therefore, this bond is much more homopolar or covalent. P and C in Fe appear to be intermediate cases between these two extremes.

These results can be easily used to describe the role that chemical bonding must play in grain boundary embrittlement. If any embrittling impurity atom such as sulfur resides in a grain boundary interstice in iron or nickel, it will draw charge off the iron or nickel atoms as it forms heteropolar bonds with them. This depletion of charge on the host metal atoms means that less charge will be available to participate in the metal-metal bonds which hold the grain boundary together. Therefore, these elements will lead to grain

boundary embrittlement. In contrast, if an impurity which is a cohesive enhancer such as boron is in the interstices of a nickel grain boundary, the charge depletion of the metal atoms will not occur. Therefore, in addition to not decreasing the charge in the metal bonds across the grain boundary, a covalent-like bond is formed between the host metal and the impurity. This bonding will give additional cohesiveness across the grain boundary.

Of course, in these small tetrahedral clusters one cannot directly observe the effect of the metal-impurity bonds on the metal-metal bonds; such an observation would require an additional shell of atoms. However, in our previous study⁽⁴²⁾ of the Ni-S system precisely such an effect was observed. The cluster used for that study contained eight atoms and is shown in Figure 13. Calculations were performed for this cluster with and without the sulfur atom in the center; nickel atoms were placed at the eight vertices. As can be seen in Figure 13, four of these nickel atoms (#1,2,3,4) were near the X-Y plane of the cluster and four were farther away (#5,6,7,8). We found that sulfur formed very strong bonds with the four nickel atoms nearest to it. This bond was again heteropolar in nature in that the charge was drawn off the nickel atoms onto the sulfur atom. The charge density contours for these two clusters are shown in Figure 14. This cross-section plot is in the X-Z plane of the cluster shown in Figure 13; it includes two of the Ni atoms near the S and two of those farther away. In the Ni_8 cluster a definite bond is formed between the nickel atoms near the center of the cluster and those farther away. When sulfur is added to the cluster, charge is drawn from the Ni atoms onto the sulfur and thus reduces the electron density available to form the metal-metal bonds. They are therefore severely weakened. This fact can be clearly seen by examining the darkened fourth contour in this figure. In the Ni_8 cluster (Figure 14a) this contour encompasses both the Ni atoms near the X-Y plane and those farther away and contributes to a bond between the two types of Ni atoms. In the Ni_8S cluster this contour has been broken into two parts. One part is now localized on the two atoms farther away from the X-Y plane and one part is now forming the Ni-S bond. However, the important point is that the bonding between the two types of atoms is severely weakened.

The model which we have described clearly shows that S should be a strong embrittler in Fe and Ni and that B should be a cohesive enhancer in Ni. These theoretical results are completely in agreement with experimental results. However, our theoretical results also suggest that phosphorus and carbon would lie between these extremes and probably would be somewhat benign elements at the grain boundary. Since this result is somewhat contrary to the perceived role of these two elements, we now examine the experimental documentation of these effects. First let us consider the role of carbon. The conclusion that carbon can counteract embrittlement comes primarily from the work of Jolly,⁽²⁾ and Pichard, Rieu, and Goux.⁽⁵⁾ They found that embrittlement in the nominally high purity iron that they were studying arose from sulfur (which had a bulk composition of approximately 35 wppm) and that carbon additions of 10-30 wppm decreased the embrittlement. However, they provided no Auger results to complement their mechanical test data. Therefore, one does not know whether carbon enhanced the cohesiveness of the boundary or whether it simply displaced the sulfur at the boundary. Our theoretical results suggest that the latter might be the case. It is clear from our calculations that even if carbon were a weak embrittler its displacement of sulfur at the grain boundary would lead to a marked improvement.

Now let us consider the data for phosphorus. Although a number of studies have been made of phosphorus embrittlement of steel,^(13,16,18,20,22) much less work has been done on iron. Because of the additional segregation of alloying elements in the steel^(19,22) one cannot assume that the embrittling potency of this element will be the same in iron and steel. However, Ramasubramanian and Stein⁽⁴⁾ did study embrittlement of iron by phosphorus and provided Auger data for this system. They found that if they doped iron with 500 to 2000 wppm of phosphorus they could get intergranular fracture and a ductile to brittle transition temperature of 150 to 200°C. However, this transition temperature did not correlate directly with the amount of phosphorus on the grain boundary and the Auger spectra from these boundaries showed the presence of sulfur and nitrogen. Furthermore, when an alloy containing 500 wppm phosphorus and 30 wppm S was tested, the ductile to brittle transition temperature went above 375°C and a much larger sulfur peak was seen on the grain boundaries. Therefore, one must conclude that phosphorus is a much weaker grain boundary embrittler than sulfur, and that the intergranular fracture observed

in these alloys could have at least partially arisen from sulfur. Therefore, our theoretical results are not contradictory to these experimental results.

Finally, we note that all of the impurity elements which we have studied are small compared to iron and nickel and should easily fit into grain boundary interstices.⁽⁵⁰⁾ However, some embrittling elements are larger than the host metal atoms—for example, Te in Fe. In these cases we would not only expect the atom to sit on a substitutional site but also that the local strain produced by the misfit would affect the bonding. Seah⁽¹²⁾ has noted that some of the strongest embrittlers in iron are atoms considerably larger than iron. Also, in addition to drawing charge out of the metal-metal bonds, the embrittling elements may change the metal-metal bond length. This result, too, could be important in embrittlement.

CONCLUSIONS

In this paper we have considered the effects of chemical bonding on grain boundary embrittlement. We have shown that a strong embrittling element such as S in Fe or Ni forms bonds with the host metal atoms around it. In doing so it draws charge from the metal atoms onto itself as it is electronegative with respect to the metal. Less charge is then available to participate in metal-metal bonds which hold the grain boundary together and embrittlement occurs. In contrast, elements which increase cohesion at the boundary such as B in Ni do not draw charge from the metal atoms but form rather covalent bonds with them. This sharing leads to increased bonding at the grain boundary. Finally, we suggest that P and C in iron are either benign or weakly embrittling and we show that existing experimental data is not inconsistent with this idea.

ACKNOWLEDGMENTS

The authors would like thank Dr. R.A. Mulford of the General Electric Research and Development Laboratory and for many discussions and for providing them with unpublished experimental data on the Ni-S and Ni-S-B systems. This

work was supported in part by the Office of the Naval Research.

Table 1

CLUSTER COMPOSITION FOR TETRAHEDRAL CLUSTERS

<u>Host Metal</u>	<u>Impurity</u>	<u>Experimentally Determined Effect of Impurities</u>	<u>Reference for Experimental Study</u>
Fe	S	Strong Embrittler	2-5, 8
Fe	P	Moderate to Weak Embrittler	4
Fe	C	Cohesive Enhancer	2,5
Ni	S	Strong Embrittler	29-32
Ni	B	Cohesive Enhancer	29

REFERENCES

1. B. E. Hopkins and H. R. Tipler, J. Iron Steel Institute, 177, 110 (1954).
2. A. Jolly, Met. Trans., 2, 341 (1971).
3. B. D. Powell, H. J. Westwood, D. M. R. Taplin, and H. Mykura, Met. Trans., 4, 2357 (1973).
4. P. V. Ramasubramanian and D. F. Stein, Met. Trans. 4, 1735 (1973).
5. C. Pichard, J. Rieu, and C. Goux, Met. Trans. A, 7A, 1811 (1976).
6. M. P. Seah and C. Lea, Phil. Mag. 31, 627 (1975).
7. J. R. Rellick, C. J. McMahon, Jr., H. L. Marcus, and P. W. Palmberg, Met. Trans. 2, 1492 (1972).
8. C. Pichard, J. Rieu, and C. Goux, Mem. Sci. Rev. Met., 70, 13 (1973).
9. C. M. Thwaites and S. K. Chatterjee, J. Iron Steel Institute, 210, 581 (1972).
10. Y. Tsukahara and A. Yoshikawa, Proc. IC STIS Supp. Trans. ISI Japan, 11, 1256 (1971).
11. J. Kameoka and C. J. McMahon, Jr., Met. Trans. A, 12A, 31 (1981).
12. M. P. Seah, Surface Science, 53, 168 (1975).
13. J. M. Capus and G. Mayer, Metallurgia, 62, 133 (1960).
14. C. J. McMahon, Jr., Mat. Sci. Eng. 25, 233 (1976).
15. R. Viswanatham and A. Joshi, Met. Trans A, 6A, 2289 (1975).
16. C. A. Hippsley, J. F. Knott, and B. C. Edwards, Acta Met., 28, 869 (1980).
17. R. Narayan and M. C. Murphey, J. Iron Steel Institute, 211, 493 (1973).
18. B. C. Edwards, H. E. Bishop, J. C. Riviere, and B. L. Eyre, Acta Met., 24, 957 (1976).
19. C. L. Briant and S. K. Banerji, Int'l. Metals Rev., 24, 164 (1978).
20. C. L. Briant and S. K. Banerji, Met. Trans. A, 10A, 1729 (1979).
21. D. L. Newhouse, American Foundrymans Soc. Trans., 85, 389 (1977).
22. R. A. Mulford, C. J. McMahon, Jr., D. P. Pope, and H. C. Feng, Met. Trans. A, 7A 1183 (1976).
23. M. Guttman, P. R. Krahe, F. Abel, G. Amsel, M. Bruneaux, and C. Cohen, Met. Trans., 5, 167 (1974).

24. J. P. Coad, J. C. Riviere, M. Guttman, and P. R. Krahe, *Acta Met.*, 25, 161 (1977).
25. J. Q. Clayton, and J. F. Knott, *Fracture 1977, ICF4*, ed. D. M. R. Taplin, Vol. 2, p. 287, Waterloo Press, Waterloo, 1977.
26. James P. Materkowski and G. Krauss, *Met. Trans. A*, 10A, 1643 (1979).
27. Wolfgang Losch, *Acta Met.*, 27, 567 (1979).
28. H. Ohtani, H. C. Feng, C. J. McMahon, Jr., and R. A. Mulford, *Met Trans A*, 7A, 87 (1976).
29. R. A. Mulford, private communication.
30. A. W. Thompson, *Grain Boundaries in Engineering Materials*, eds. J. L. Walter, J. H. Westbrook and D. A. Woodford, p. 607, Claitors Publishing Division, Baton Rouge, LA (1974).
31. R. T. Holt and W. Wallace, *Int. Metals. Rev.*, 21, 1 (1976).
32. M. G. Lozinskiy, G. M. Volkogen, and N. Z. Pertsovskiy, *Russ. Metall.*, 5, 65 (1967).
33. E. D. Hondros and D. McLean, *Phil. Mag.* 29, 771 (1974).
34. D. McLean and L. Northcott, *J. Inst. Metals*, 72, 583 (1946).
35. D. McLean, *J. Inst. Metals*, 81, 121 (1952).
36. H. L. Marcus and N. E. Paton, *Met. Trans.*, 5, 2135 (1974).
37. J. H. Bechtold and B. J. Shaw, *Fracture*, ed. H. Liebowitz, Vol. 6, p. 371, Academic Press, New York (1969).
38. A. Joshi and D. F. Stein, *Met. Trans.*, 1, 2543 (1970).
39. Wolfgang Losch, *Acta Met.*, 27, 1885 (1979).
40. H. Ohtani, H. C. Feng, and C. J. McMahon, Jr., *Met. Trans. A*, 7A, 1123 (1976).
41. R. G. Rowe, *Met. Trans. A*, 10A, 997 (1979).
42. C. L. Briant and R. P. Messmer, *Phil. Mag. B*, 42, 569 (1980).
43. J. C. Slater, *Advances in Quantum Chemistry*, ed. P. O. Lowden, Vol. 6, p. 1, Academic Press, New York (1972).
44. K. H. Johnson, *Advances in Quantum Chemistry*, ed. P. O. Lowden, Vol. 7, p. 143, Academic Press, New York (1973).
45. M. F. Ashby, F. Spaepen, and S. Williams, *Acta Met.*, 26, 1647 (1978).
46. R. C. Pond, D. A. Smith and V. Vitek, *Acta Met.*, 27, 235 (1979).
47. A. J. Bennett, B. McCarroll, and R. P. Messmer, *Phys. Rev. B*, 3, 1397 (1971).

48. R. P. Messmer and D. R. Salahub, Phys. Rev. B, 16, 3415 (1977).
49. R. P. Messmer, Phys. Rev. B, 23, 1616 (1981).
50. H. J. Frost, M. F. Ashby, and F. Spaepen, Scripta Met., 14, 1051 (1980).

FIGURE CAPTIONS

- Figure 1: The tetrahedron. The metal atoms (M) are placed at the vertices and the impurity (I) in the center. The cross hatched plane is the one used for the contour plots shown in this paper.
- Figure 2: The energy level diagram for the Fe_4S cluster.
- Figure 3: The energy level diagram for the Ni_4S cluster.
- Figure 4: The energy level diagram for the Fe_4P cluster.
- Figure 5: The energy level diagram for the Fe_4C cluster.
- Figure 6: The energy level diagram for the Ni_4B cluster.
- Figure 7: The orbital contour plots of the $1a_1$ and $1t_2$ orbitals in Fe_4S .
- Figure 8: The orbital contour plots of the $1a_1$ and $1t_2$ orbitals in Ni_4S .
- Figure 9: The orbital contour plots of the $1a_1$ and $1t_2$ orbitals in Fe_4P .
- Figure 10: The orbital contour plots of the $1a_1$ and $1t_2$ orbitals in Fe_4C .
- Figure 11: The orbital contour plots of the $1a_1$ and $1t_2$ orbitals in Ni_4B .
- Figure 12: The special charge density $\rho_{\text{IM}}(r)$ for the tetrahedral clusters. These charge densities include only those orbitals which contain a contribution from the impurity atom.
- Figure 13: The eight atom tetragonal dodecahedron.
- Figure 14: Contour values of the total valence charge density in the X-Z plane of the tetragonal dodecahedron shown in Figure 13. (a) is for Ni_8 and (b) is for Ni_8S . Contour four which differs most drastically for the two clusters is drawn more darkly.

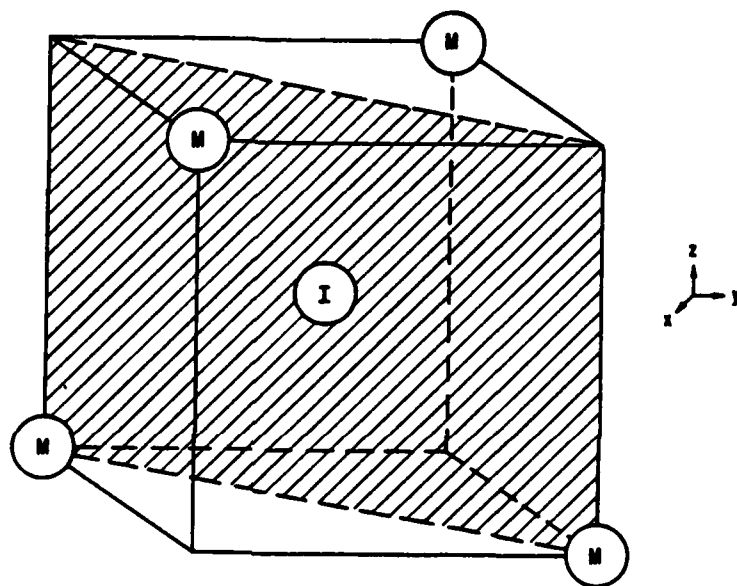


Fig. 1

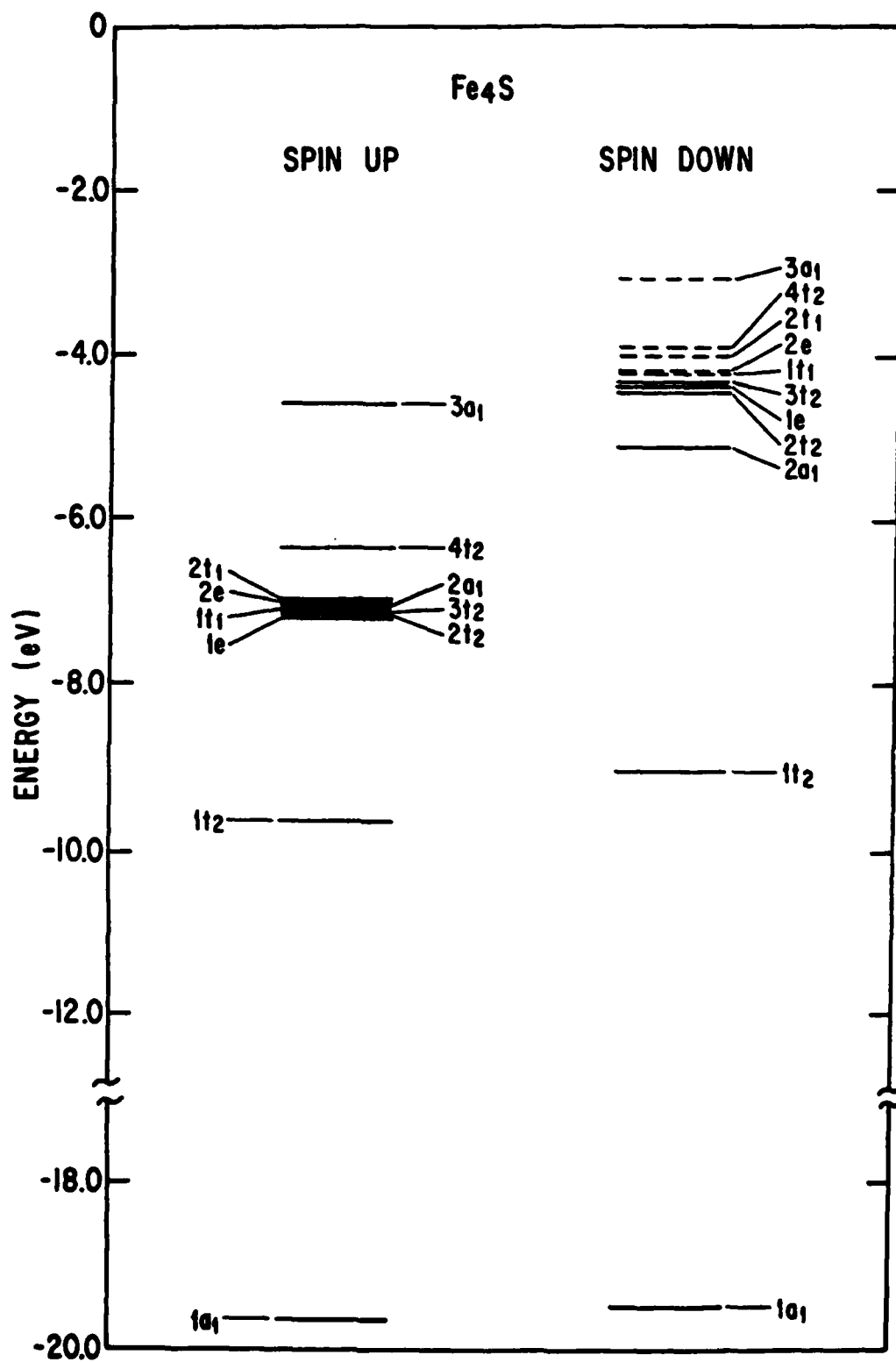


Fig. 2

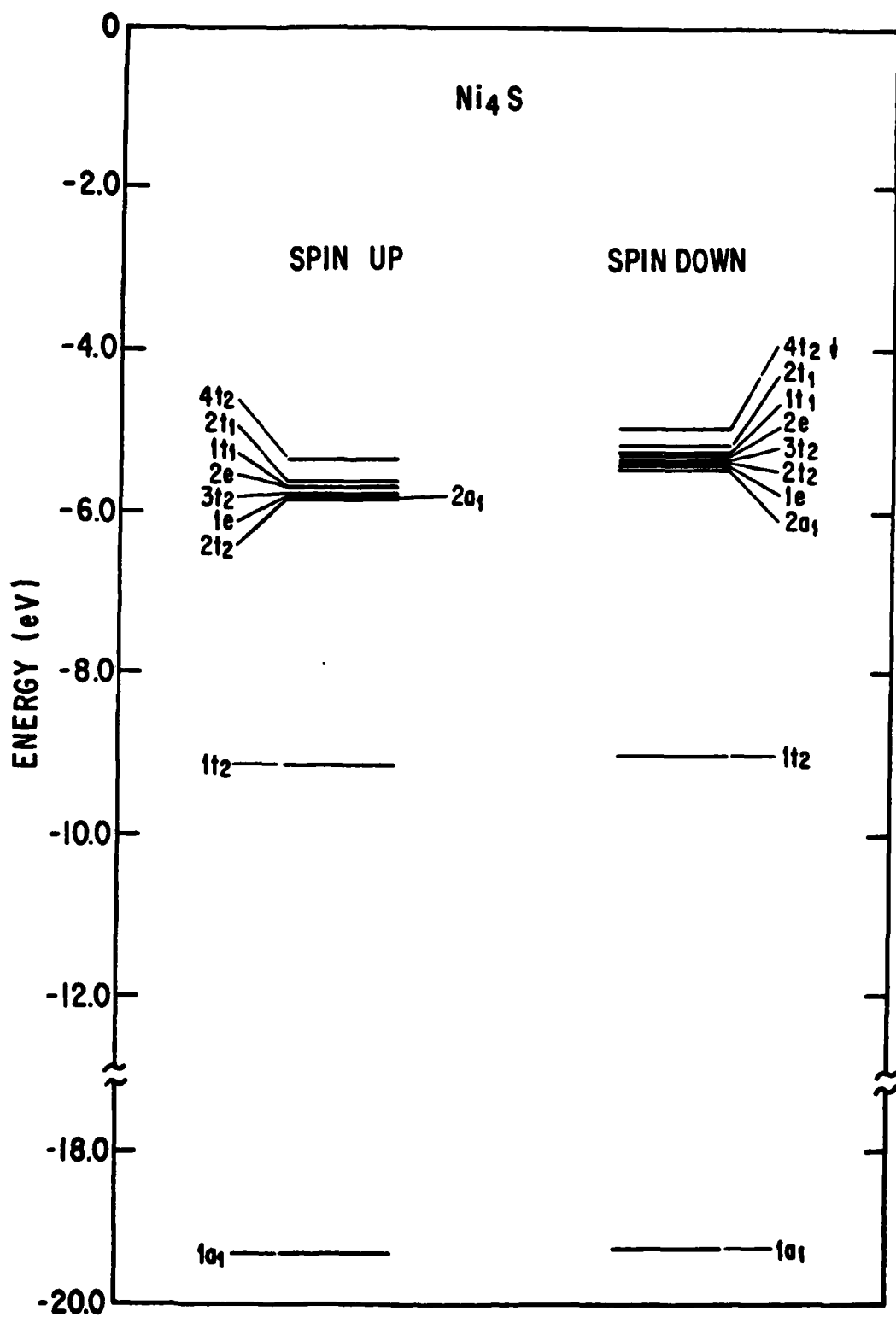


Fig. 3

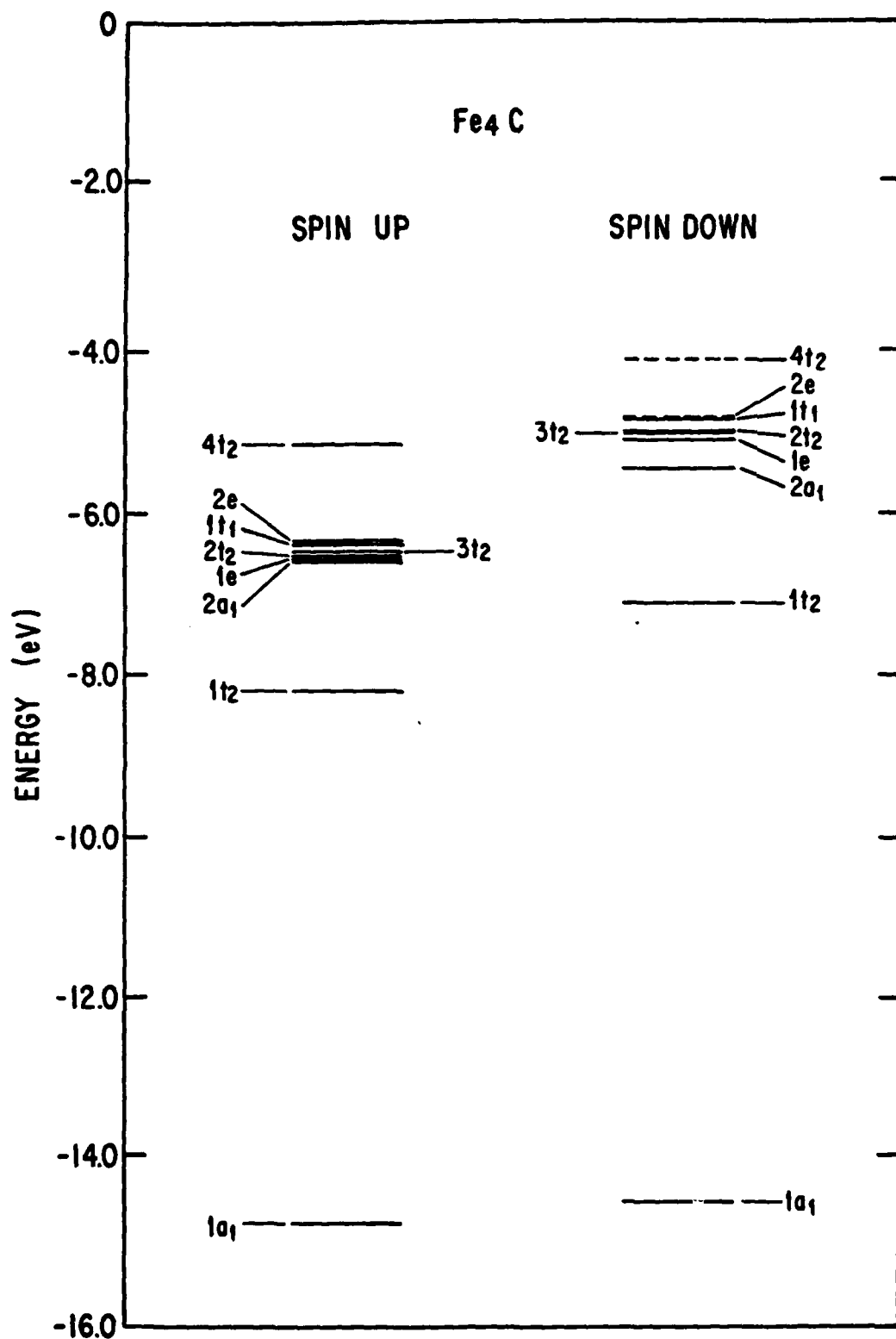


Fig. 5

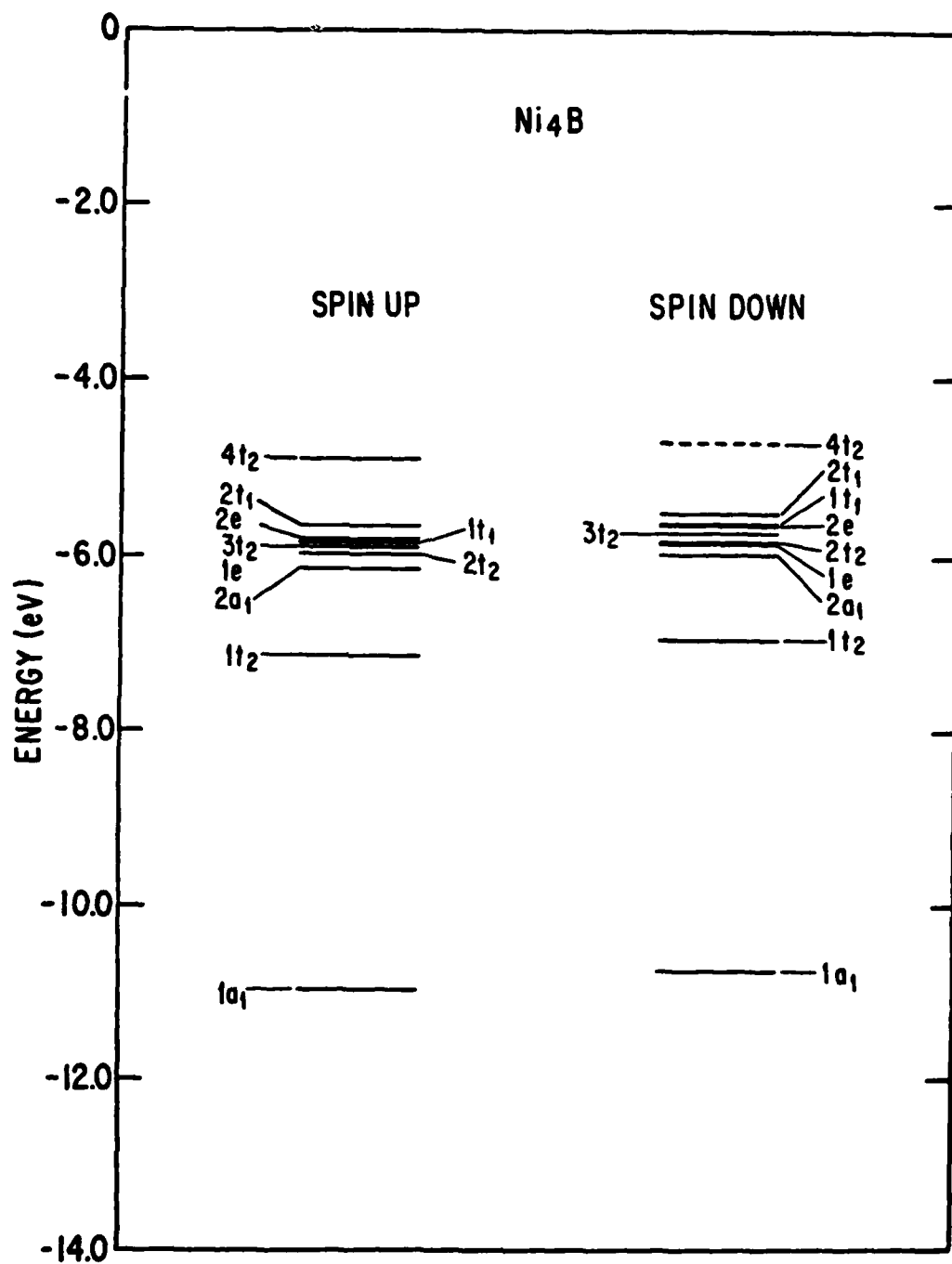
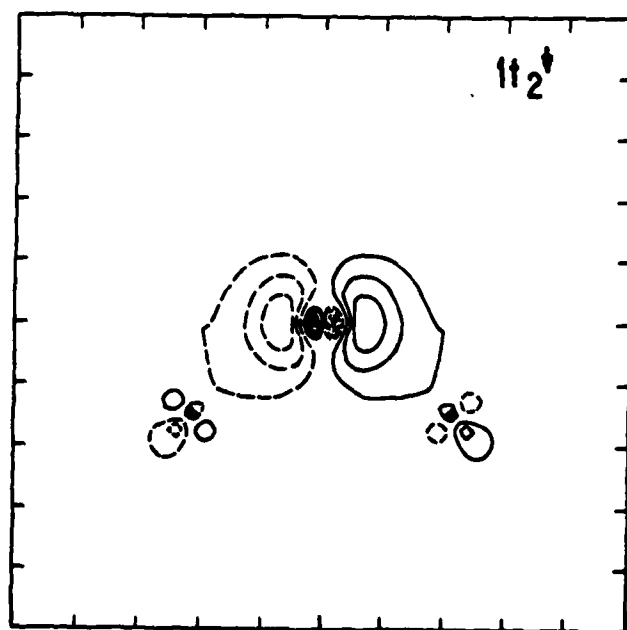
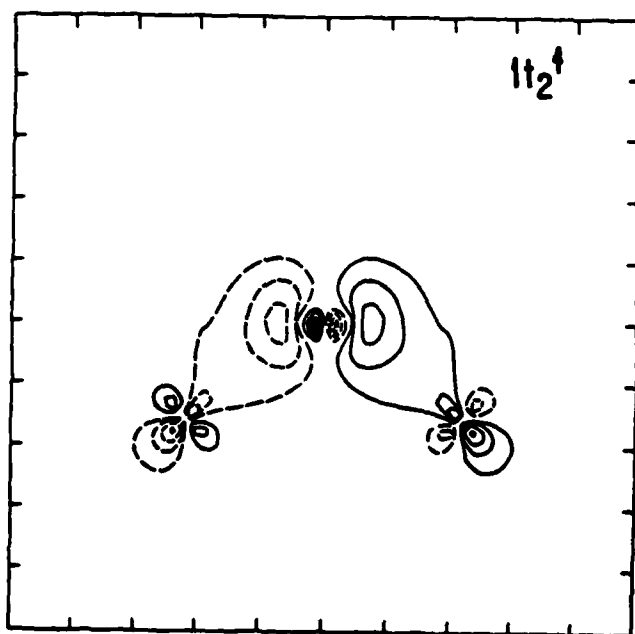
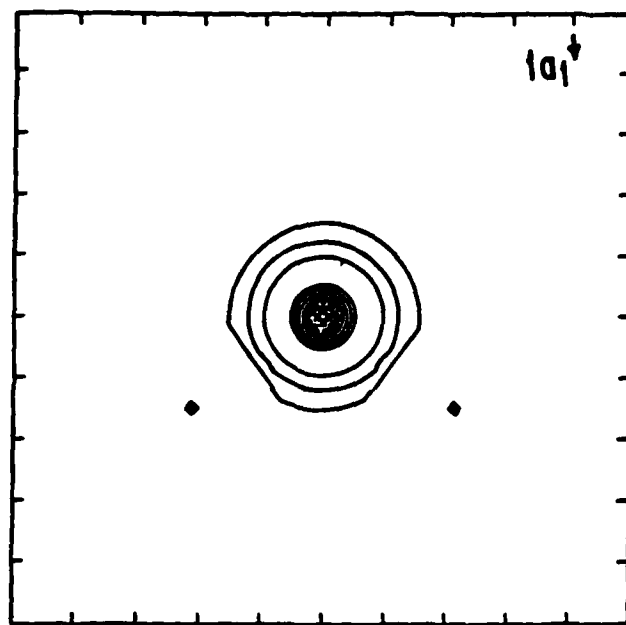
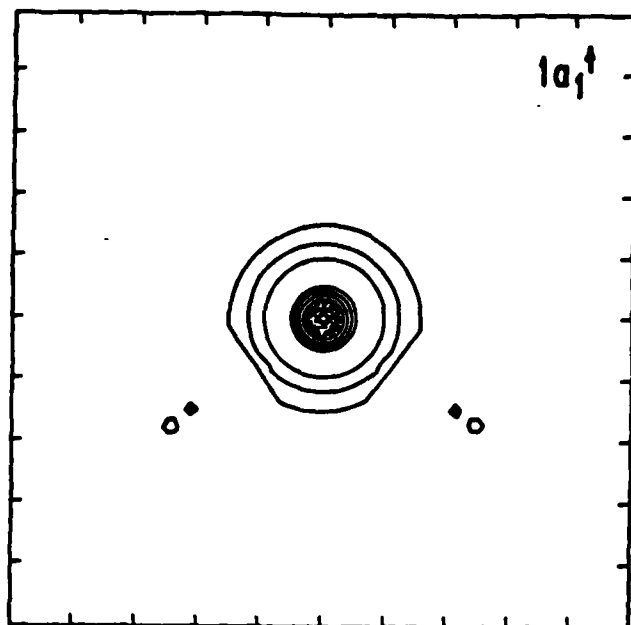


Fig. 6

Fe_4S



Ni_4S

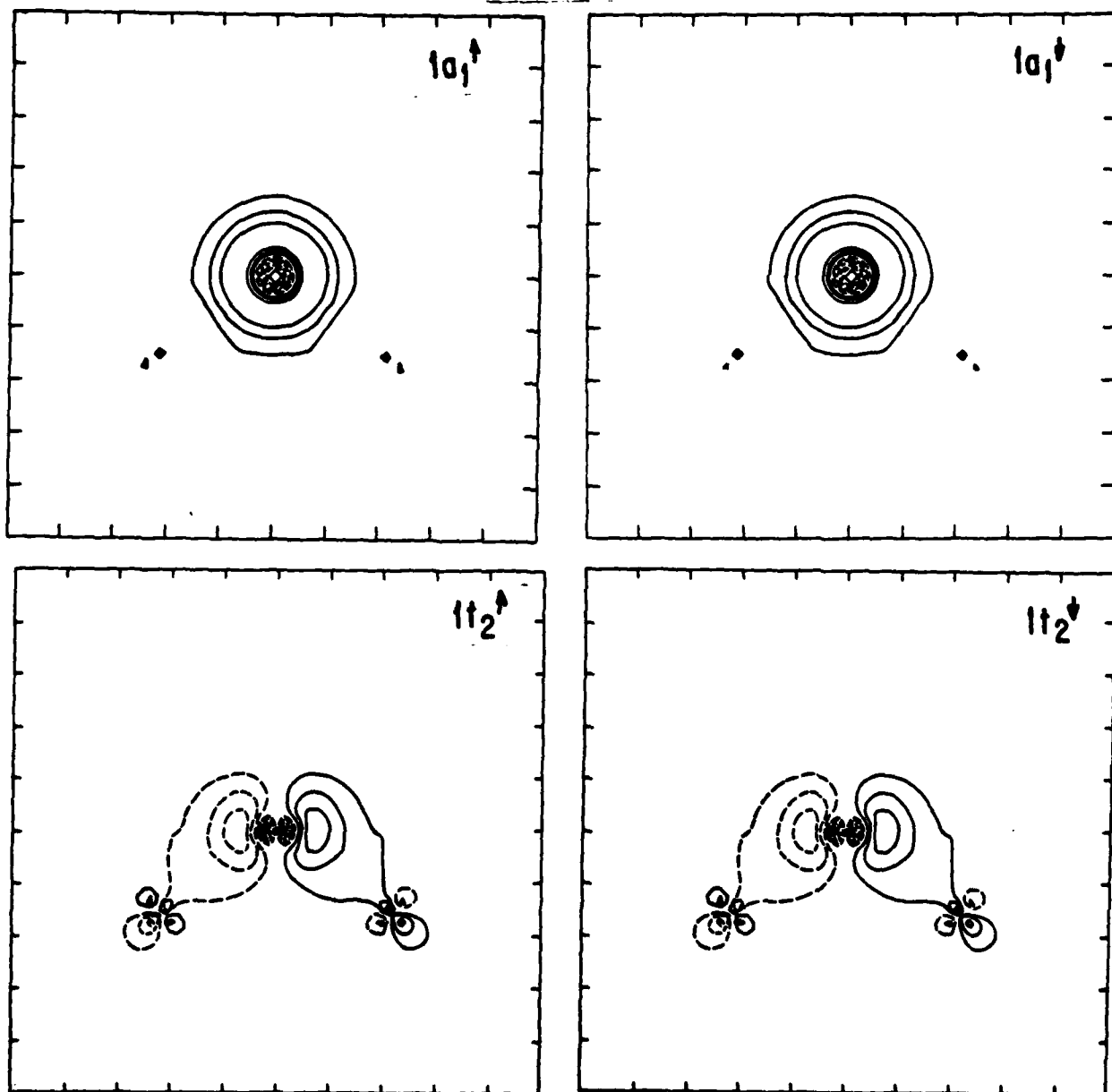


Fig 8

Fe_4P

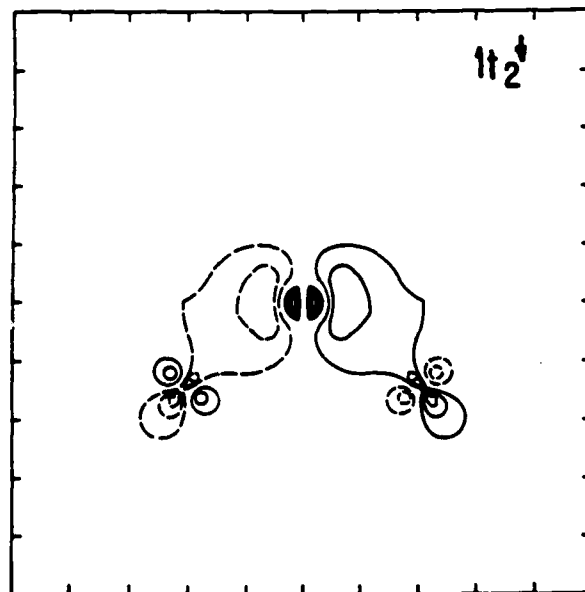
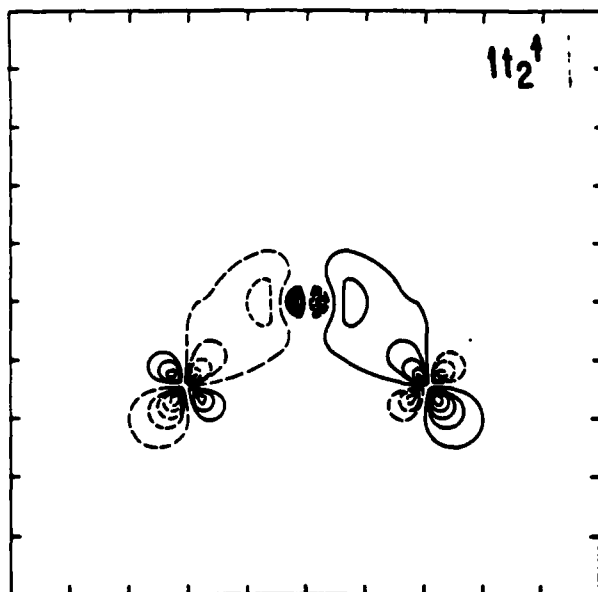
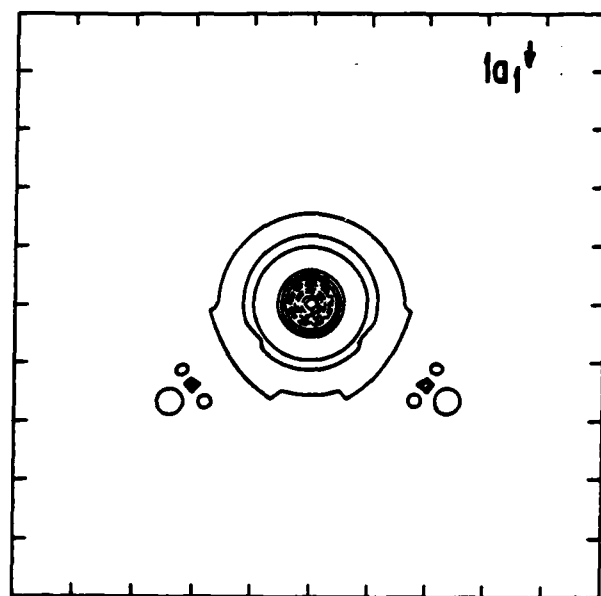
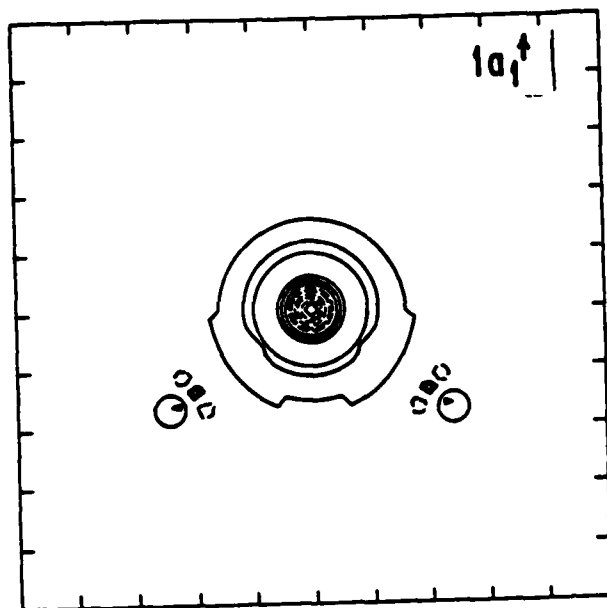


Fig.

Fe_4C

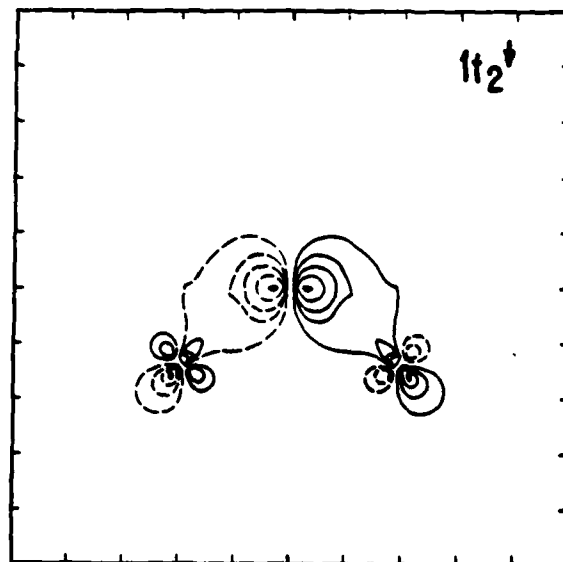
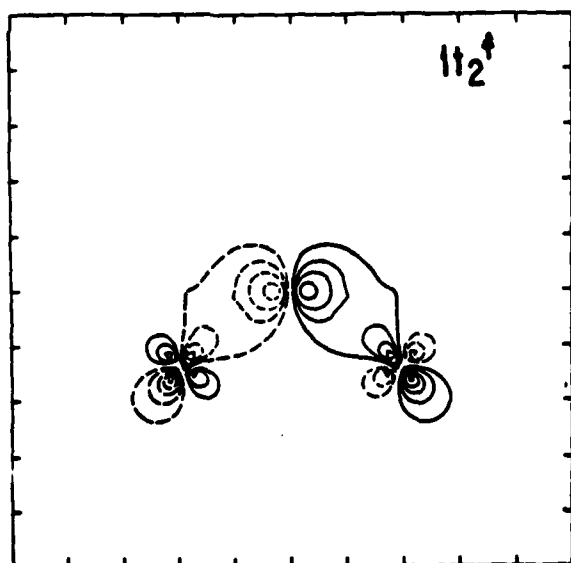
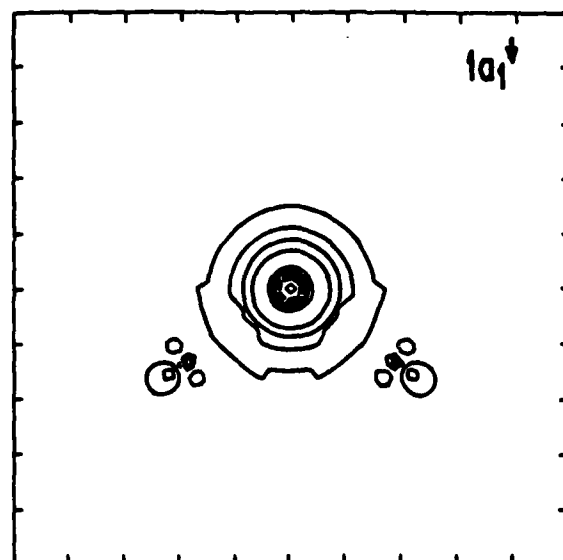
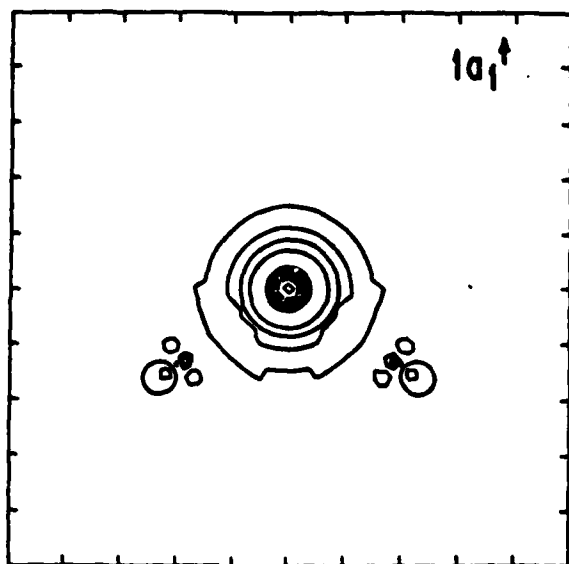


Fig 10

Ni_4B

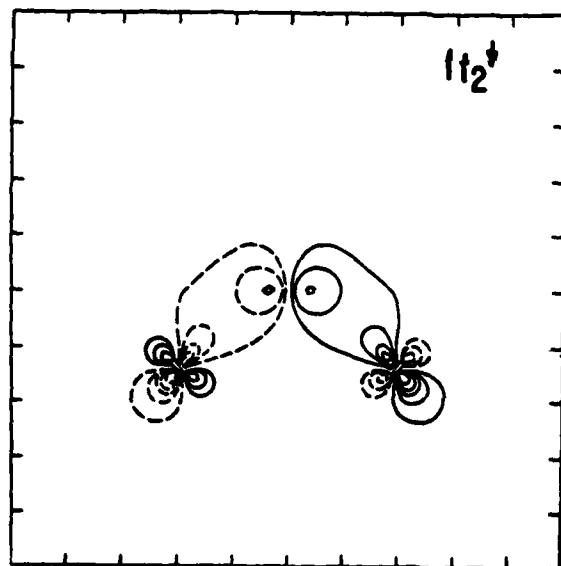
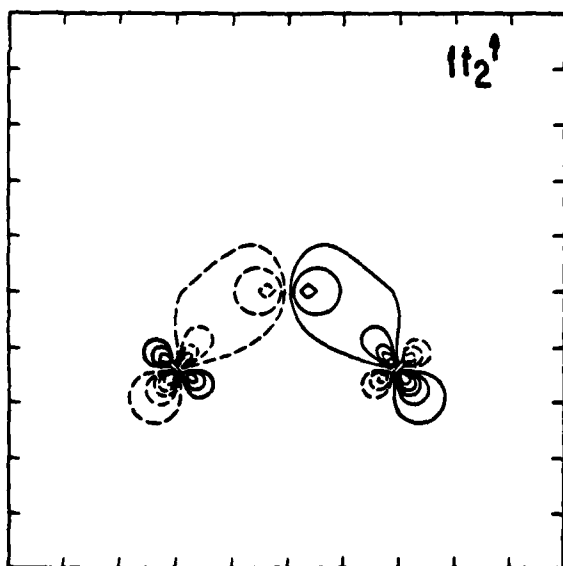
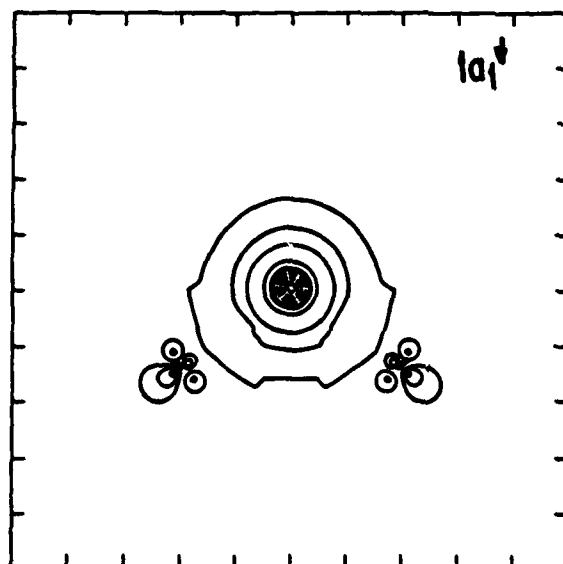
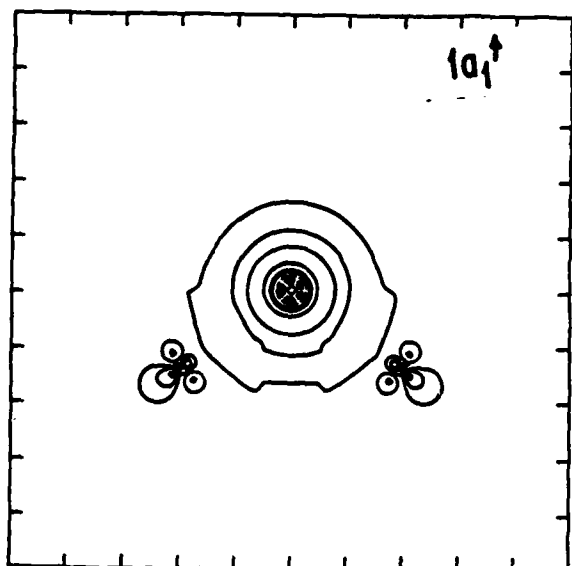


Fig. 11

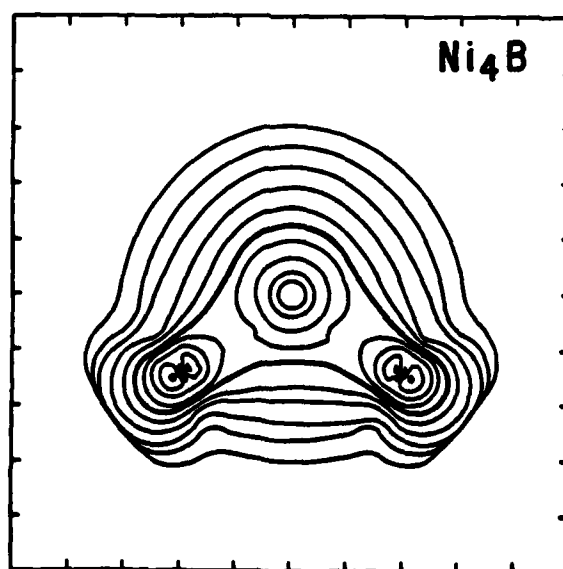
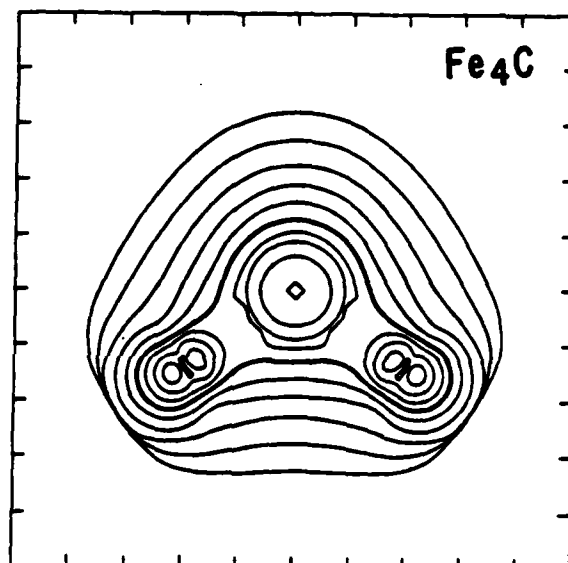
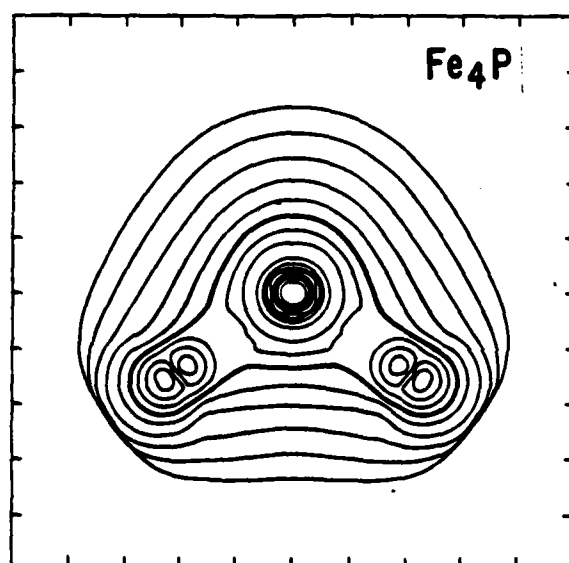
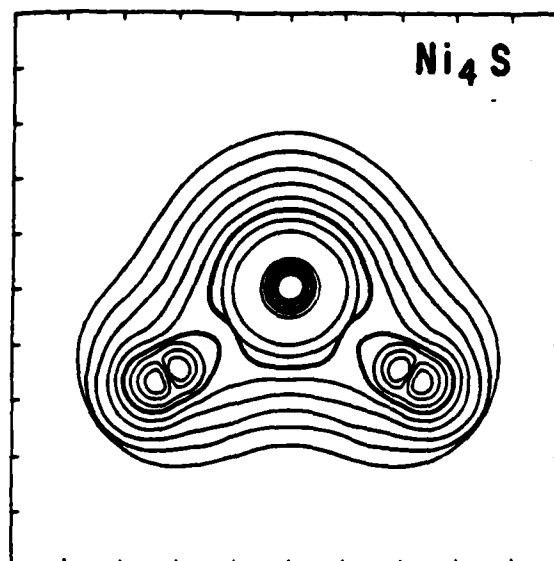
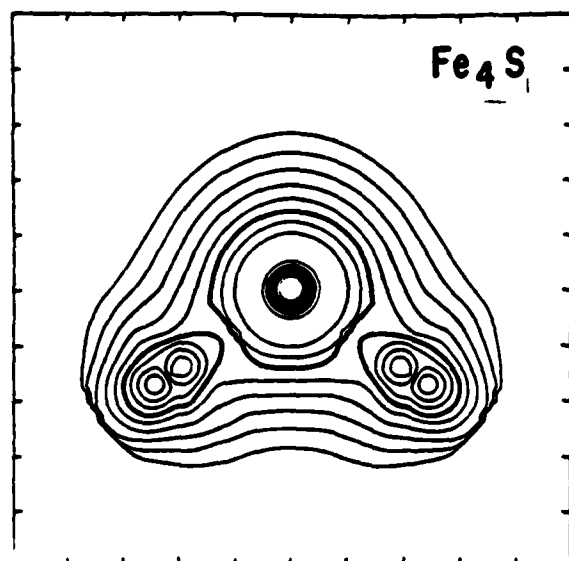
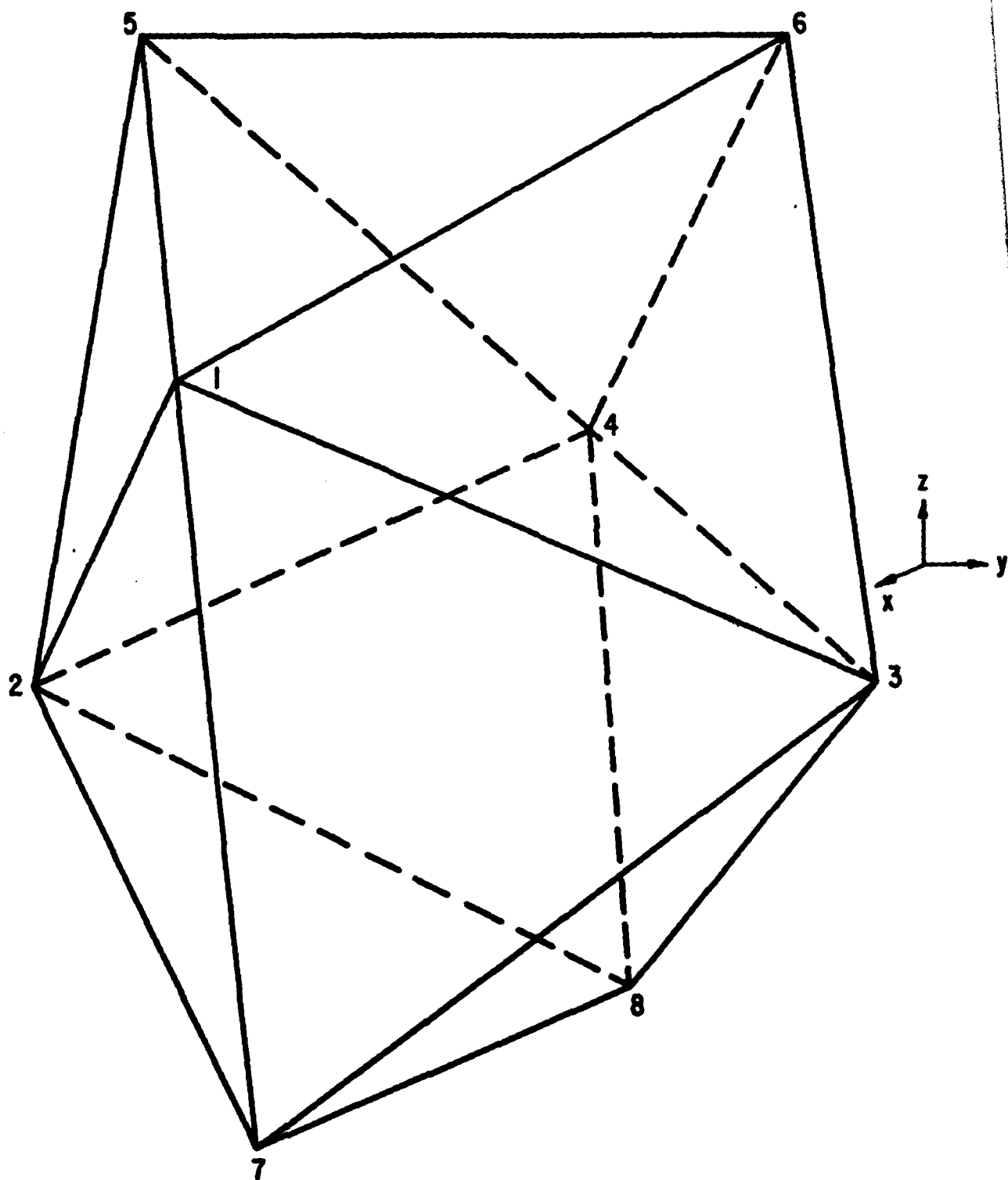


Fig. 12



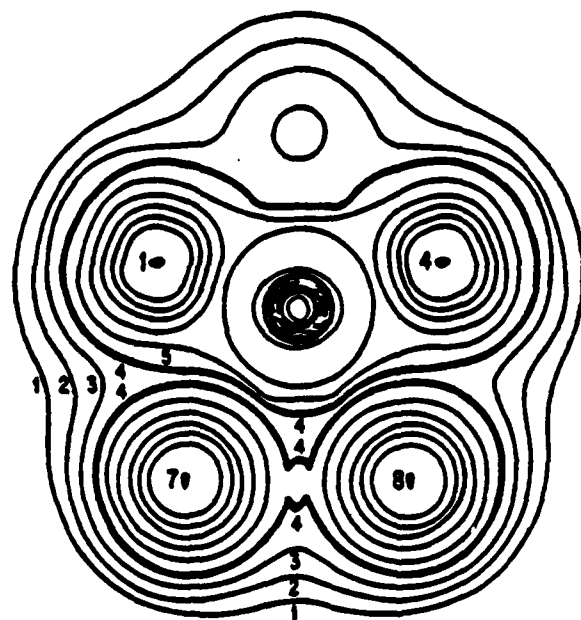
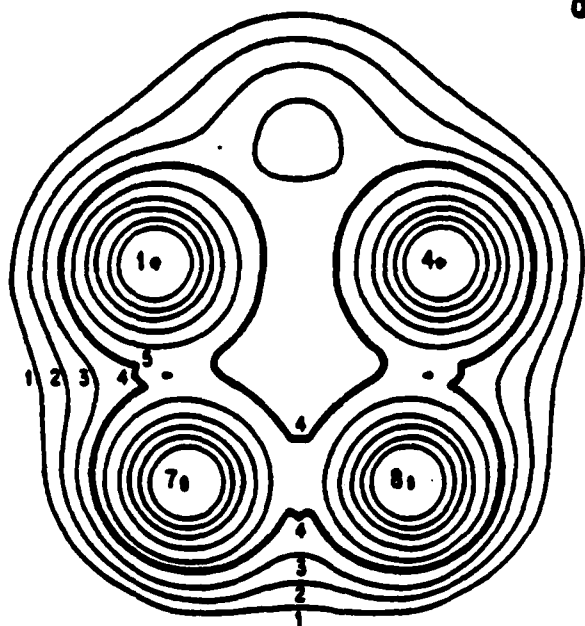


Fig 14